THE ASTROPHYSICAL JOURNAL, 400:351–361, 1992 November 20

RAPID TIME VARIATIONS AND RADIATIVE INSTABILITIES OF ASTROPHYSICAL MASERS

GERARDO A. SCAPPATICCI AND WILLIAM D. WATSON
Department of Physics, University of Illinois at Champaign-Urbana, Urbana, IL 61801
Received 1992 January 28; accepted 1992 May 23

ABSTRACT

The time-varying intensities are obtained for astrophysical masers that are radiatively unstable. Numerical integrations of the time-dependent, nonlinear equations of radiative transfer are performed with the usual approximation of a linear maser. At long times after changes in the physical conditions, the intensity of maser radiation reaches an asymptotic behavior and oscillates permanently in these idealized calculations with a period that is related to the length of the maser divided by the speed of light. The intensity varies by more than a factor of 10. These intensities depend upon the same four parameters as we originally found to determine the regime for radiative instabilities based on a stability analysis of the steady state. A detailed comparison is made between the predictions of the stability analysis and the time variations of the intensities. Calculations are performed for interacting pairs as well as isolated, individual masers.

In realistic astrophysical environments, a number of considerations can be expected to reduce significantly the variation in the radiation that is observed, and to mask or prevent a periodic time dependence of this radiation. Radiative instabilities may be present in the 1665 MHz OH masers for which fluctuations in the intensity have recently been reported on time scales as short as 10^3 s.

Subject headings: instabilities — masers — radiative transfer

1. INTRODUCTION

In early observations of masers in astrophysics, significant variations in intensity were found to occur on time scales as short as days. Though none were reliably identified, this led to theoretical investigations for possible radiative instabilities in astrophysical masers. Salem & Middleton (1978) performed the most detailed study and numerically integrated the time-dependent equations for the radiative transfer and molecular populations (see Bettweiser 1979; Deguchi 1974; Nedoluha 1990). Relaxation oscillations following perturbations were found in these calculations. In all cases that were examined, however, the oscillations died away after only a few periods. Recurrent fluctuations of $\sim 10\%$ in the intensity of interstellar 1665 MHz OH masers on time scales down to 1000 s have now been reported by Clegg & Cordes (1991, and private communication). As discussed by these investigators, the fluctuations are believed to be intrinsic to the masers and not due to interstellar scintillation. Representative estimates for the dimensions of these masers are in the neighborhood of 10^{14} cm. Hence, the time scale for variations due to hydrodynamical motions would be expected to be ~ 1 yr (order of magnitude) and much longer than the observed fluctuations. In contrast, the characteristic time scale for radiative instabilities would be the light crossing time and is comparable with the shortest times found in the observations. The fluctuations were not found in 1665 MHz OH masers that are located in circumstellar regions.

We have thus undertaken to reexamine the radiative stability of astrophysical masers. This investigation was begun in a previous publication (Scappaticci & Watson 1992a, b, hereafter SW) in which radiative instabilities were found for plausible physical conditions for the 1665 MHz OH masers. These are found by performing a stability analysis for small (linear) perturbations to the steady state solutions for the properties of linear masers. The occurrence of the instabilities, as well as the properties of the time-dependent maser intensities computed in §§ 2 and 3, are found to depend upon four dimensionless parameters. One of these ($\Gamma L/c$) relates the phenomenological decay constant Γ for the molecular excitations to the length L of the maser and must be near one for instabilities in an isolated maser. This reflects the essence of the instability. When a maser is radiatively saturated so that the molecular populations depend upon the intensity of the maser radiation, the strongly nonlocal nature of the radiative transport leads to relaxation oscillations with a period L/c following a perturbation. The oscillations are caused by a competition between the radiation propagating in opposite directions and is aided by the regions of exponential amplification for the incoming radiation at the ends of the maser. They occur even when the relaxation time ($1/\Gamma$) for the molecular populations in the rate equations is so short that at any instant, steady state populations can be assumed to be applicable (i.e., $dn/dt = 0$ in eqs. [1] and [2]). When the period of these oscillations corresponds to the time scale for the relaxation of the molecular populations ($\Gamma L/c \simeq 1$), a resonance occurs and perturbations can grow instead of die away. SW found that other requirements must also be satisfied for perturbations to grow (instability). A significant region of exponential amplification is needed. It is measured by a parameter β (see eq. [12]), and to some extent by the degree of saturation which is controlled mostly by the optical depth parameter τ (see eq. [8]). The degree of saturation must also be large enough that the molecular populations are influenced sufficiently by the maser radiation. Partial saturation is necessary for instability, but heavy saturation restores stability. Spontaneous emission tends to quench radiative instabilities through its contribution in the radiative transfer equations. Because it is proportional to the molecular population and not to the population difference as is the amplification, the contribution of spontaneous emission is insensitive to the fluctuations in intensity that drive the instability. The relative importance of spontaneous emission for quenching the instability is proportional to the frequency of the radiation divided by the brightness temperature of the continuum radiation that is incident onto the maser. It is this factor that leads

us to conclude that these radiative instabilities are less likely in the SiO and H_2O masers, which occur at much higher frequencies than 1665 MHz. The incident radiation ordinarily is also weaker at the higher frequencies.

The stability analysis of SW makes it possible to see that there are radiative instabilities and under what conditions they occur. It does not describe the maser after a perturbation grows and is no longer small. The stability analysis does not thus provide information on how far the maser intensities might deviate from the steady state values nor, necessarily, on their time variation in this regime. Obtaining this information by the numerical integration of the full nonlinear, time-dependent equations for the radiative transfer and molecular populations is the purpose of the investigation here.

In § 2 we consider the time-dependent properties of a single linear maser and in § 3, the properties of two such masers which interact through their maser radiation. Separated masing components that interact have been envisioned as a cause for the extreme surface brightness of certain masers (Deguchi & Watson 1989). In both sections, we compare in detail the predictions of the stability analysis with the numerical solutions that we obtain for the time-dependent intensities. The idealization of a linear maser is utilized in all calculations. This ordinarily is a satisfactory approximation because of the high degree of beaming of maser radiation. We believe that it is satisfactory for the purposes here. The relationship of the calculations to the observations is discussed in § 4.

2. SINGLE MASERS

2.1. *Time Variations*

The masing transition is treated in the common, two-level approximation in which the interaction with other molecular states is approximated by "phenomenological" pumping rates Λ and decay rates Γ. We have, in addition, performed limited calculations in which all four of the energy levels involved in the 18 cm transitions are included. No significant differences were found in the regimes of parameter space that were considered. The rate equations for the populations *per magnetic substate* and per unit volume of the upper (u) and lower (l) states of the masing transition are

$$\frac{\partial n_u}{\partial t} = \Lambda_u - \Gamma n_u - R(n_u - n_l) - An_u \tag{1}$$

for the upper state and

$$\frac{\partial n_l}{\partial t} = \Lambda_l - \Gamma n_l + \frac{g_u}{g_l} R(n_u - n_l) + \frac{g_u}{g_l} An_u \tag{2}$$

for the lower state. Here, g_u and g_l are the statistical weights of the two states, R is the rate for stimulated emission from the upper to the lower state, and A is the Einstein coefficient for a transition from the upper to the lower state through spontaneous emission.

In general, equations (1) and (2) must be solved as a function of molecular velocity because the rate for stimulated emission varies across the spectral line. The spectral line profile for the radiation and hence the velocity dependence of the stimulated emission also changes along the length of the maser. If, however, the rate for the relaxation of the molecular velocities (not explicitly included in these equations) is greater than the rate for stimulated emission, the molecular velocity distribution remains Maxwellian despite the effect of stimulated emission. Equations (1) and (2) can then be solved without considering any deviation of the populations from a Maxwellian distribution. Goldreich & Kwan (1974) have reasoned that the relaxation of molecular velocities in OH 18 cm masers by trapped infrared radiation is rapid enough that the masing molecules do retain a Maxwellian velocity distribution. The observation that the spectral line profiles of intense OH masers commonly are narrow tends to support this reasoning. We thus assume that the relaxation of molecular velocities is rapid enough that the interaction with the maser radiation does not alter the shape of the velocity distribution of the OH molecules The n_u and n_l in equations (1) and (2) can then be interpreted as total populations obtained by integration over velocity. When an explicit form is needed for the velocity distribution, we approximate it by a rectangular distribution having a full width Δv. It follows that we also approximate the spectral line profile of the maser radiation by a rectangular profile with a full width of v_0 ($\Delta v/c$), where v_0 is the central frequency of the maser transition. We regard the use of rectangular distributions for the molecular velocities and radiation to have negligible influence on the results (this had been verified in a limited number of cases). In contrast, the assumption that the relaxation of molecular velocities is faster than the rate for stimulated emission has a major impact. In the opposite limit, the instabilities that we find would not seem to occur. The equation for the radiative transfer to the intensity I_ν of maser radiation at frequency ν is given by

$$\frac{dI_\nu}{ds} - \kappa_\nu I_\nu + \epsilon_\nu , \tag{3}$$

where the distance s is in the direction of propagation of the radiation and the total derivative contains the time derivative. For the rectangular profile for the molecular velocities,

$$\kappa_\nu = g_u B_{ul}(n_l - n_u)hc/4\pi\,\Delta v , \tag{4}$$

$$\epsilon_\nu = g_u n_u Ahc/4\pi\,\Delta v , \tag{5}$$

where $B_{ul}(=c^2A/2h\nu^3)$ is the Einstein coefficient for stimulated emission from the upper to the lower state.

We now rearrange the foregoing equations from their familiar form into a form that is convenient for the calculations here. The maser radiation is considered to propagate along the x-axis so that the intensities and molecular populations depend upon x and time t. Maser radiation can propagate in both directions along the x-axis. The intensities are expressed in terms of the brightness temperatures $T_\pm(x, t)$ of the radiation propagating in the positive and negative directions ($T_\pm = c^2 I_{\nu,\pm}/2\nu^2 k$) normalized by the brightness temperature T_0 of the background, continuum radiation that is incident upon the maser. We thus designate $\tilde{T}_\pm(\tilde{x}, \tilde{t}) = T_\pm(\tilde{x}, \tilde{t})/T_0$ so that, in explicit time-dependent form, equation (3) becomes

$$\frac{\partial \tilde{T}_+}{\partial \tilde{t}} + \frac{\partial \tilde{T}_+}{\partial \tilde{x}} = \tau\left[\rho\tilde{T}_+ + \left(\frac{h\nu}{2kT_0}\right)\rho + \left(\frac{h\nu}{2kT_0}\right)\rho_s\right], \tag{6}$$

$$\frac{\partial \tilde{T}_-}{\partial \tilde{t}} - \frac{\partial \tilde{T}_-}{\partial \tilde{x}} = \tau\left[\rho\tilde{T}_- + \left(\frac{h\nu}{2kT_0}\right)\rho + \left(\frac{h\nu}{2kT_0}\right)\rho_s\right] \tag{7}$$

for the maser radiation propagating in the two directions. In these equations, the time and distance are replaced by the normalized quantities $\tilde{t} = t/(L/c)$ and $\tilde{x} = x/L$ for a masing region of length L. The optical depth parameter is

$$\tau = g_u\left(\frac{c^3}{8\pi\nu^3}\right)\frac{A}{\Delta v}\frac{\Delta\Lambda}{\Gamma}L , \tag{8}$$

where $\Delta\Lambda = \Lambda_u - \Lambda_l$ is the net inversion in the pumping. Normalized molecular populations and population differences are given, respectively, by

$$\rho_s = \Gamma(n_u + n_l)/\Delta\Lambda = \Lambda/\Delta\Lambda = \text{constant}\ , \tag{9}$$

where $\Lambda = \Lambda_u + \Lambda_l$ and

$$\rho(\tilde{x}, \tilde{t}) = \Gamma(n_u - n_l)/\Delta\Lambda\ . \tag{10}$$

Combining and rearranging equations (1) and (2) in a similar manner yields

$$\frac{\partial\rho}{\partial\tilde{t}} = \left(\frac{\Gamma L}{c}\right)\left\{1 - [1 + \beta(\tilde{T}_+ + \tilde{T}_-)]\rho - \frac{A}{\Gamma}\rho - \frac{A}{\Gamma}\rho_s\right\} \tag{11}$$

which depends upon $\tilde{x}$ and $\tilde{t}$. For the OH 1665 MHz transition, $g_u = g_l$. This simplification has been incorporated into equation (11). The additional parameter

$$\beta = \frac{1}{2\pi}\frac{kT_0}{h\nu}\frac{A}{\Gamma}\Delta\Omega \tag{12}$$

introduces the angle $\Delta\Omega$ into which the maser radiation is beamed. It is taken to be constant in the calculations presented here. To obtain an indication of the sensitivity of the results to this idealization, we did perform computations elsewhere (SW) in which $\Delta\Omega$ has a plausible variation. No qualitatively significant difference is evident. Including an estimate for $\Delta\Omega$ in the calculations is essential for a realistic relationship between the intensity and the rate of stimulated emission in a linear maser (e.g., Nedoluha & Watson 1991).

Including spontaneous emission frequently has negligible influence in calculations for the properties of astrophysical masers. Its contribution here is reflected by the terms in equations (6) and (7) that contain the factor $(h\nu/2kT_0)$ and in equation (11), by the terms that contain (A/Γ) explicitly. The influence of spontaneous emission in the rate equation (11) is, in fact, always negligible in our calculations. However, we find that it plays a key role through equations (6) and (7) in quenching the radiative instability when the fractional inversion in the pumping $\Delta\Lambda/\Lambda$ is small enough.

When $\Delta\Lambda/\Lambda$ is sufficiently large that spontaneous emission can be ignored, the solutions for the brightness temperatures $\tilde{T}_\pm$ of the radiation that emerges from the maser depend upon three parameters—τ, β, and $\Gamma L/c$. If spontaneous emission is important, the solutions also depend upon a fourth parameter $(h\nu/2kT_0)\Lambda/\Delta\Lambda$. We have previously shown that the steady state solutions to equations (6), (7), and (11) are unstable for certain values of these parameters (SW). We now wish to investigate how the solutions behave in the nonlinear regime where the previous analysis based on small (or linear) perturbations is no longer valid. To do this, the initial conditions must be specified. It is natural either to specify the way in which the maser is "turned on," or to start from steady state solutions and to specify how they are perturbed. Although we have obtained similar solutions by both approaches, we focus on calculations in which the maser is turned on with the full time dependence. The maser is started by turning on the pumping which is accomplished by replacing $\Delta\Lambda$ by $\Delta\Lambda f(\tilde{t})$ in the original rate equations. This has the effect in the final equations of replacing equation (11) by

$$\frac{\partial\rho}{\partial\tilde{t}} = \left(\frac{\Gamma L}{c}\right)\left\{f(\tilde{t}) - [1 + \beta(\tilde{T}_+ + \tilde{T}_-)]\rho - \frac{A}{\Gamma}\rho - \frac{A}{\Gamma}\rho_s\right\} \tag{13}$$

To start the time-dependent calculations presented here, either $f(\tilde{t})$ is immediately set to one ("instantaneous" turn on) or

$$f(\tilde{t}) = 1 - \exp\,[-(\tilde{t}/\tilde{t}_0)^2] \tag{14}$$

with $\tilde{t}_0 = 10$ to 100. At $\tilde{t} = 0$, ρ is set to zero and $\tilde{T}_+ = \tilde{T}_- = 1$ everywhere. Calculations with even larger $\tilde{t}_0$ have not been performed because of the limitations of computer cpu time. Those with $\tilde{t}_0 = 100$ are sufficient to demonstrate that unstable behavior can be initiated by changes in the physical conditions of the maser which have characteristic variations that are much slower than the resulting unstable fluctuations.

If Figure 1, we present the solutions of the foregoing equations for these three starting conditions and for representative values of the parameters β, τ, and $\Gamma L/c$ in the unstable region. Permanent oscillations in the maser radiation are found that can be as large as a factor of 100. In addition, the solutions for the emergent maser radiation become identical after a long time regardless of how the maser is started. With minor exceptions, which will be discussed subsequently, we have always found this to be the case for the much wider range of values of the relevant parameters that we have investigated. We have also performed computations for which $f(\tilde{t})$ in equation (14) is given a dependence on $\tilde{x}$ while retaining $f(\tilde{x}, \tilde{t}) \to 1$ for the large $\tilde{t}$. No qualitatively significant new features were evident. The main result that is found from changing the way in which the masing is initiated in Figure 1 is that the asymptotic solutions that are obtained after a long time are reached much more slowly for large $\tilde{t}_0$. This presumably reflects the ability of the system to respond more nearly adiabatically to slow changes. Hence the "perturbation," which is the difference between the actual and the steady state values of $\tilde{T}_\pm$ and ρ, is much smaller. A long time is thus required for it to grow to the asymptotic solutions. Since the asymptotic solutions are the same for the different initial conditions and are obtained much more quickly (in computer time) with the instantaneous turning on of the maser, we focus on these in most of the calculations presented in the figures.

In Figures 2–6, we provide an indication of how the asymptotic solutions for the maser radiation depend upon the essential parameters $-\tau$, β, ρ_s, $\Gamma L/c$, and any asymmetry in the incident continuum radiation. Instability requires that the maser be partly but not heavily, radiatively saturated as demonstrated in Figure 2 (see also SW). At both the smallest and largest values of τ in this figure, where $R/\Gamma \simeq 4$ and 20, respectively, the initial perturbation dies away because the steady state solution is stable. The unstable regime in which the oscillations are permanent extends over a range of about a factor of 2 in τ, or a factor of 4 in R/Γ. This can be interpreted as a factor of 2 in the length L of the maser or in the pump rate $\Delta\Lambda$. Although calculations are shown for only one choice of β and $\Gamma L/c$ (with $\rho_s = 0$), this range in τ for the instability regime is representative of our more extensive computations. When the parameter β is larger than $\sim 2 \times 10^{-8}$, the instability is quenched as indicated in Figure 3. For different choices of other parameters, this limit for β can be somewhat smaller (SW). The relationship between the intensity of the radiation and the rate for stimulated emission is governed by β. It determines the relative size of the region in which each beam grows exponentially with distance. If this region is larger, instability tends to be more likely. With A and ν for the 1665 MHz masing transition of OH, $\beta = 1.4 \times 10^{-9}[(T_0/100\ \text{K})(\Delta\Omega/10^{-4}\ \text{sr})(0.001\ \text{s}^{-1}/\Gamma)]$. Although we return in § 4 to discuss likely

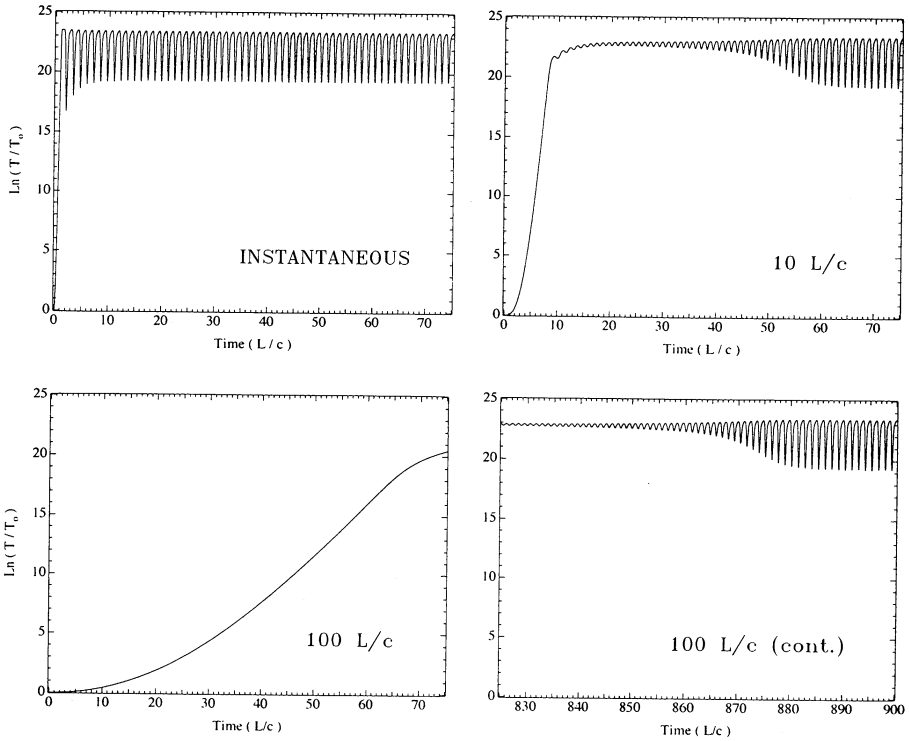

FIG. 1.—Representative intensities of radiation that emerges from a maser (expressed as the natural logarithm of the brightness temperature of the maser divided by that of the incident radiation T_0) as a function of time in units of the length L of the maser divided by the speed of light. Intensities are shown that result when the pumping for the maser is turned on instantaneously, and over characteristic time scales of $10L/c$ and $100L/c$ (see text for details). Here $\beta = 2 \times 10^{-9}$, $\Gamma L/c = 1.25$, and $\tau = 55(R/\Gamma \simeq 8)$.

values for the physical quantities that determine β, we note that very small beaming angles $\Delta\Omega$ seem plausible in view of recent evidence that $\Delta\Omega$ are as small as 10^{-5} sr for some astrophysical water masers (Nedoluha & Watson 1991). As spontaneous emission becomes relatively more important in comparison with the incident continuum radiation, the instabilities are quenched at some point. The solutions for the maser radiation presented in Figure 4 illustrate the influence of spontaneous emission which depends upon the quantity $(h\nu/2kT_0)\rho_s$. To specify ρ_s in Figure 4, we adopt $\nu = 1665$ MHz and $T_0 = 100$ K. With these choices, the instabilities tend to be quenched when $\rho_s \gtrsim 100$. This limit for ρ_s is insensitive to the values of β, τ, and $\Gamma L/c$. The quantity $(h\nu/2kT_0)\rho_s$ is also the ratio of the magnitude of the excitation temperature and T_0. When this ratio exceeds ~ 0.1, the maser is stable. In the calculations here, the instability also is quenched when the intensities incident onto the opposite ends of the maser differ by more than a factor of ~ 2 (see Fig. 5).

2.2. *Linear Stability Analysis*

Further insight and confidence in the reliability of the conclusions can be derived by closely comparing the foregoing calculations with expectations from a stability analysis of the steady state solutions. This is done in Figure 6. The stability analysis is performed as in SW. With $\tilde{T}^0_{\pm}(\tilde{x})$ and $\rho^0(\tilde{x})$ as the steady state solutions, we substitute the functions $\tilde{T}^0_{\pm}(\tilde{x}, \tilde{t}) = \tilde{T}^0_{\pm}(\tilde{x}) + \delta T_{\pm}(\tilde{x}, \tilde{t})$ and $\rho(\tilde{x}, \tilde{t}) = \rho^0(\tilde{x}) + \delta\rho(\tilde{x}, \tilde{t})$ into equations (6), (7), and (11). As is then standard in a linear stability analysis, we determine whether there are growing solutions for the small perturbations $\delta\tilde{T}_{\pm}$ and $\delta\rho$ that are proportional to $e^{w\tilde{t}}$. That is, solutions for which the real part of w is positive are unstable for small or "linear" perturbations. With these substitutions, the linearized forms of the previous equations are

$$\mp \frac{d[\delta\tilde{T}_{\pm}(\tilde{x})]}{d\tilde{x}} + [\tau\rho^0(\tilde{x}) - w]\delta\tilde{T}_{\pm}(\tilde{x}) + \tau\left[\tilde{T}^0_{\pm}(\tilde{x}) + \left(\frac{h\nu}{2kT_0}\right)\right]\delta\rho(\tilde{x}) = 0\,, \quad (15)$$

$$\delta\rho(\tilde{x}) = \frac{-\beta[\delta\tilde{T}_{+}(\tilde{x}) + \delta\tilde{T}_{-}(\tilde{x})]\rho^0(\tilde{x})}{\{w/(\Gamma L/c) + 1 + \beta[\tilde{T}^0_{+}(\tilde{x}) + T^0_{-}(\tilde{x})] + A/\Gamma\}}\,. \quad (16)$$

The solution thus requires first obtaining the steady state functions $\tilde{T}^0_{\pm}(\tilde{x})$ and $\rho^0(\tilde{x})$. Equations (15) and (16) are then solved by numerical integration to obtain the eigenvalues w subject to the boundary conditions $\delta\tilde{T}_{+}(0) = 0$ and $\delta\tilde{T}_{-}(1) = 0$. For small small enough deviations from the steady state solutions that the linear equations remain valid, the period for the time dependent oscillation is given by 2π divided by the imaginary part of the eigenvalue w. At least for the ranges of parameters that we consider, we have found that there are only two eigenvalues that can have Re $(w) > 0$ for a single maser. We designate these as w_0 and w_0^*. These modes are symmetric.

In Figure 6, we compare the results of these calculations for w_0 with the intensities of the radiation as a function of time from the same masers obtained using the methods of § 2.1. The time-dependent solutions are in excellent agreement with expectations from the stability analysis. When $\Gamma L/c$ is near one and Re $(w_0) > 0$, the oscillations of the time-dependent intensities are permanent. For both larger and smaller $(\Gamma L/c)$, the time-dependent solutions relax to the steady state intensities as is expected because Re $(w_0) < 0$ for these $\Gamma L/c$. In addition, the periods for oscillation in intensity are near, but slightly larger

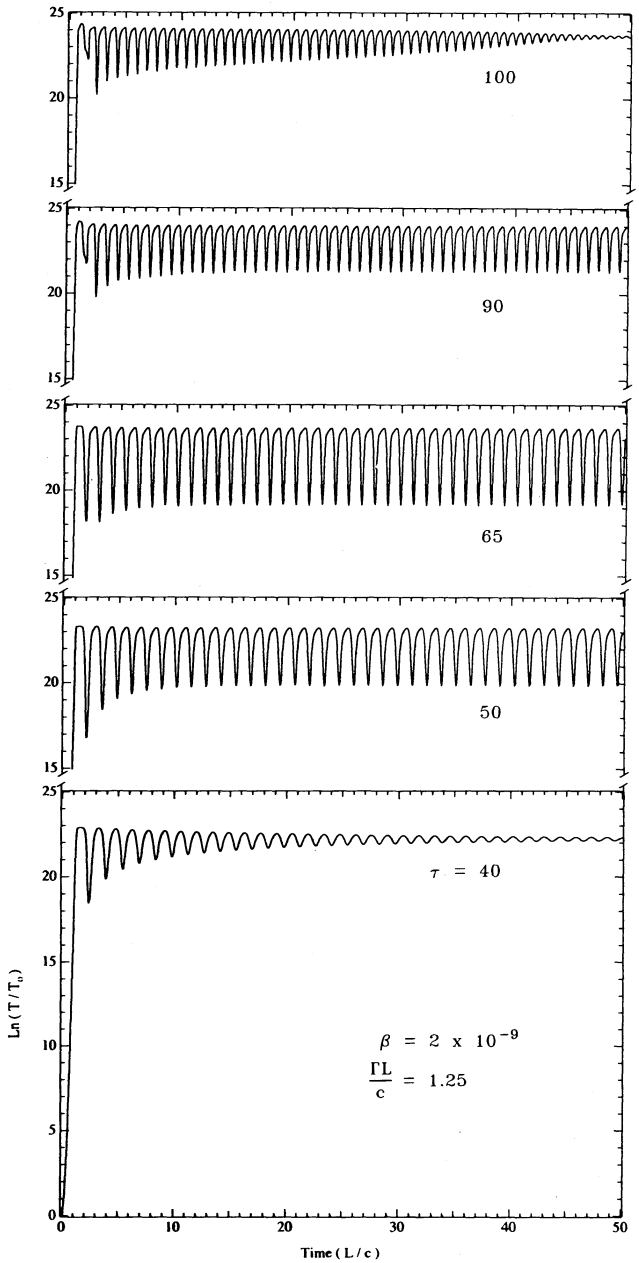

FIG. 2.—Similar to Fig. 1. Here the influences of the degree of saturation on the emergent intensities in indicated by varying the optical depth parameter τ. The degree of saturation ranges from $R/\Gamma \simeq 4$ ($\tau = 40$) to $R/\Gamma \simeq 20$ ($\tau = 100$). The pumping for the maser is turned on instantaneously at time zero.

than, (L/c) as is the period found in the stability analysis. Both tend to become longer as $\Gamma L/c$ decreases. This general agreement between these two methods for assessing the instability of masers is representative of numerous other choices for the relevant parameters. Further examples of this agreement are given in § 3 for pairs of interacting masers.

3. PAIRS OF INTERACTING MASERS

We now assess the radiative instability of pairs of masers that interact with one another through their maser radiation. Two identical linear masers are positioned with their axes along a common line so that the radiation passes through both masers. For the examples in this section, the value of the optical depth parameter for each maser is $\tau = 25$. Hence, the intensity of maser radiation that emerges from the pair of masers in steady state is exactly the same as for a single maser with $\tau = 50$. In all examples of this section, the length L represents the distance between the outer ends of the two masing regions. That is, it is the distance between the location at which background, continuum radiation enters one maser and the location at which the radiation emerges on the far side of the other masing region.

In Figure 7, we present the time variation of the brightness temperature of the maser radiation that emerges from a pair of masers for representative choices of the values of the relevant parameters. The masing is initiated by turning on the pumping $\Delta\Lambda$ in the same manner as for the computation in Figure 1. Regardless of whether the masing is initiated instantaneously or slowly in a characteristic time as long as $t_0 = 100L/c$, the solutions for the emergent radiation becomes identical after a long time. As in the case of the single maser, we can then examine the properties of the asymptotic (as a function of time)

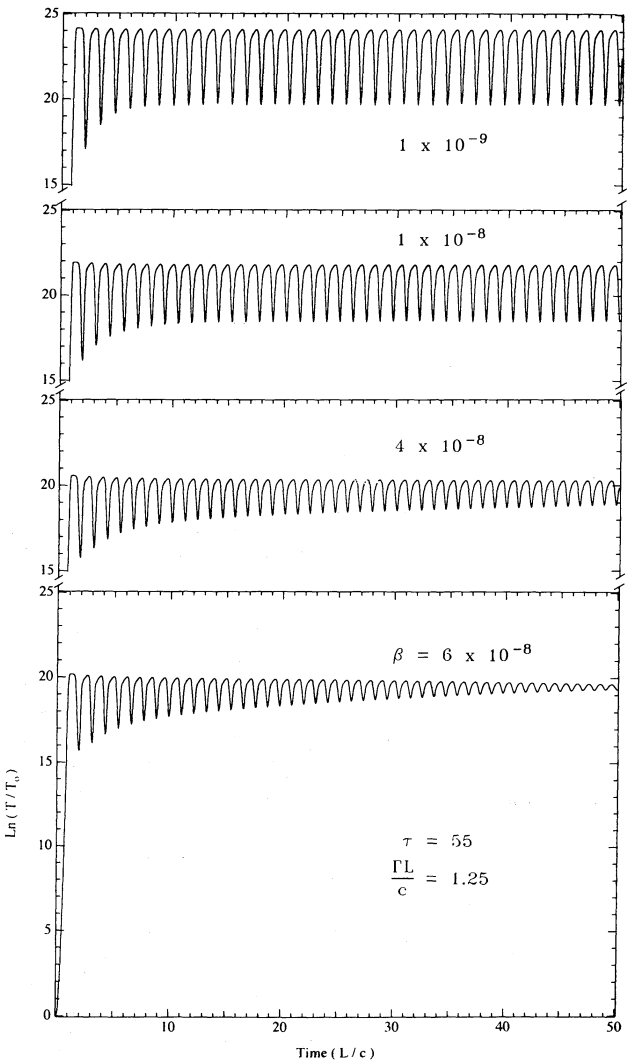

FIG. 3.—Similar to Figs. 1 and 2. Here the dependence of the intensity of the emergent maser radiation on the parameter β is indicated ($\beta = kT_0 A \Delta\Omega/2\pi h\nu\Gamma$). The pumping is turned on instantaneously ($R\Gamma \simeq 10$).

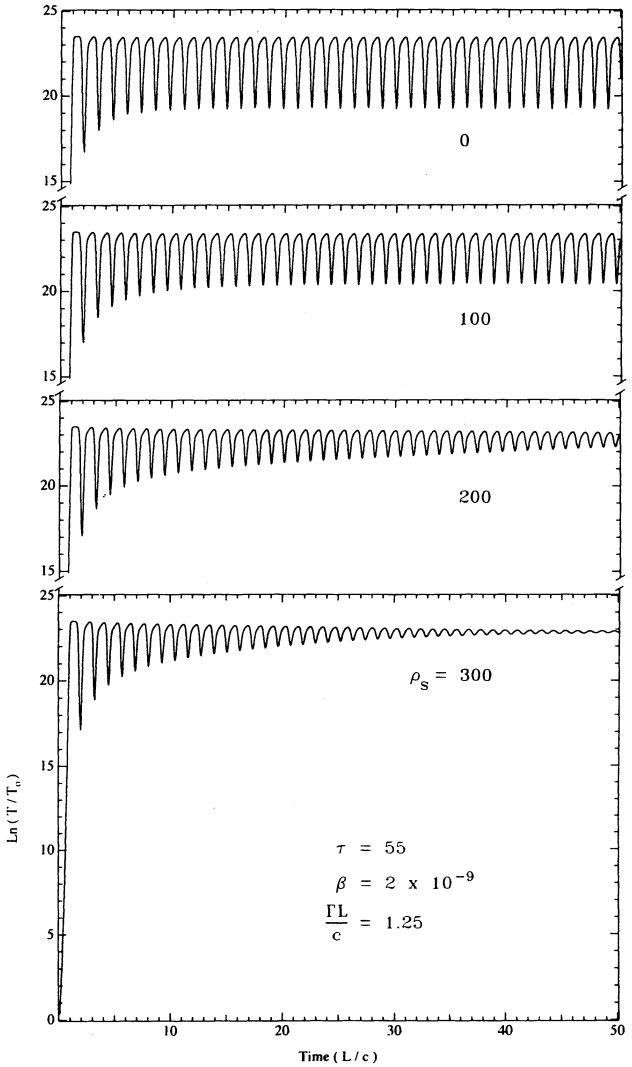

FIG. 4.—Similar to Figs. 1 and 2 except that here the dependence of the emergent maser radiation on the contribution of spontaneous emission is examined (ρ_s is the inverse of the fractional inversion of the pumping). For these calculations $T_0 = 100$ K and $\nu = 1665$ MHz. The pumping is turned on instantaneously ($R/\Gamma \simeq 10$).

solutions without considering how the masing is begun. The irregular variations of the brightness temperature which occur before the asymptotic solutions are reached is of potential interest. For the slower and perhaps most realistic changes in the masing gas due to external perturbations, the time to reach the permanent, periodic oscillations is quite long. External perturbations may occur on a similar time scale so that the periodicity expected from the asymptotic solutions may not be reached before another external perturbation alters the maser again. The evolution of the maser begun with $t_0 = 100L/c$ is also noteworthy because it appears to reach a different asymptotic solution in Figure 7*j*; it subsequently begins to switch modes (Fig. 7*k*) and ultimately reaches the same asymptotic solution as for the other two starting conditions. The periodicities of these variations can be related to those of modes that are identified in the linear stability analysis shown in Figure 8.

When the linear stability analysis described in the previous section is applied to these interacting pairs of masers, a number of eigenvalues can have Re $(w) > 0$ and can thus be unstable. The number seems to increase with the separation between the masing components. We limit our attention to symmetric eigenmodes because only these have been excited in our time-dependent calculations. We suspect that unstable antisymmetric modes also exist. In Figures 8, 9, and 10, we compare the results of these calculations for Re (w) with the asymptotic solutions for the emergent maser radiation obtained by integrating the time-dependent equations as for Figure 7. In Figure 8, the configuration of the masing components is the same as for the calculations of Figure 7—each masing component has a length of $0.1L$. The separation between inner edges of the components is the $0.8L$. As in the analogous comparison for a single maser (Fig. 6), there is excellent agreement in Figure 8 between the predictions from the stability analysis and the results from the time-dependent calculations for the brightness temperatures. When $\Gamma L/c = 25$ at which no eigenvalues have Re $(w) > 0$, the oscillations die away and the asymptotic solution for the brightness temperature is constant. At $\Gamma L/c$ of 5 and 15 where there are Re $(w) > 0$, the brightness temperature has permanent oscillations. Regardless of how the masing is started in Figure 7, the system ultimately chooses the mode with a period of $0.6L/c$

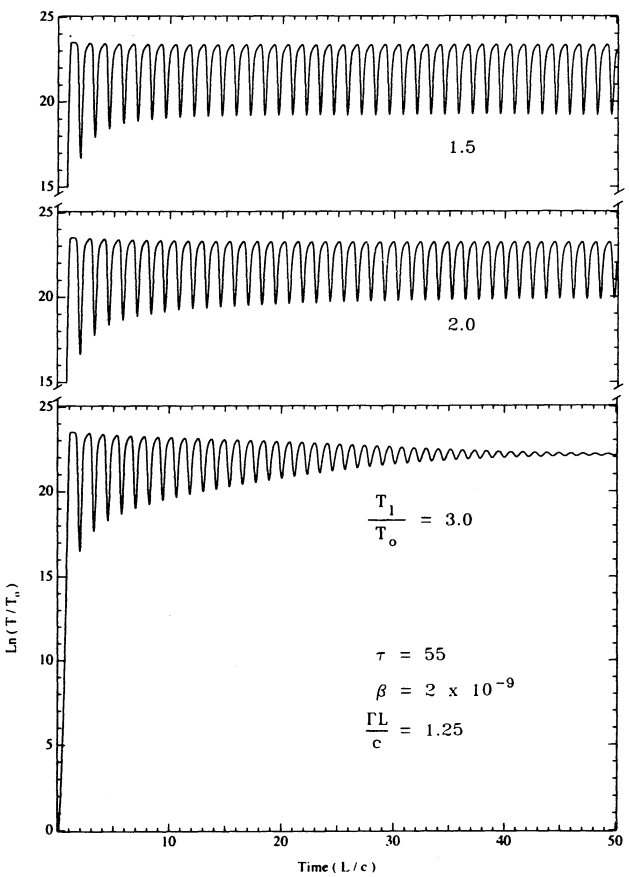

FIG. 5.—Similar to Figs. 1 and 2 except that here the sensitivity of the emergent maser radiation to unequal intensities of continuum radiation incident at the ends of the maser is examined. The brightness temperature at one end is larger than at the other by the factor T_1/T_0 specified in the figure. The natural logarithm of the brightness temperature of the emergent radiation that propagates in the same direction as the smaller of the two incident intensities is shown. The pumping is turned on instantaneously and $R/\Gamma \simeq 4$ for $T_1/T_0 = 3$ and $R/\Gamma \simeq 10$ for $T_1/T_0 = 1.5$.

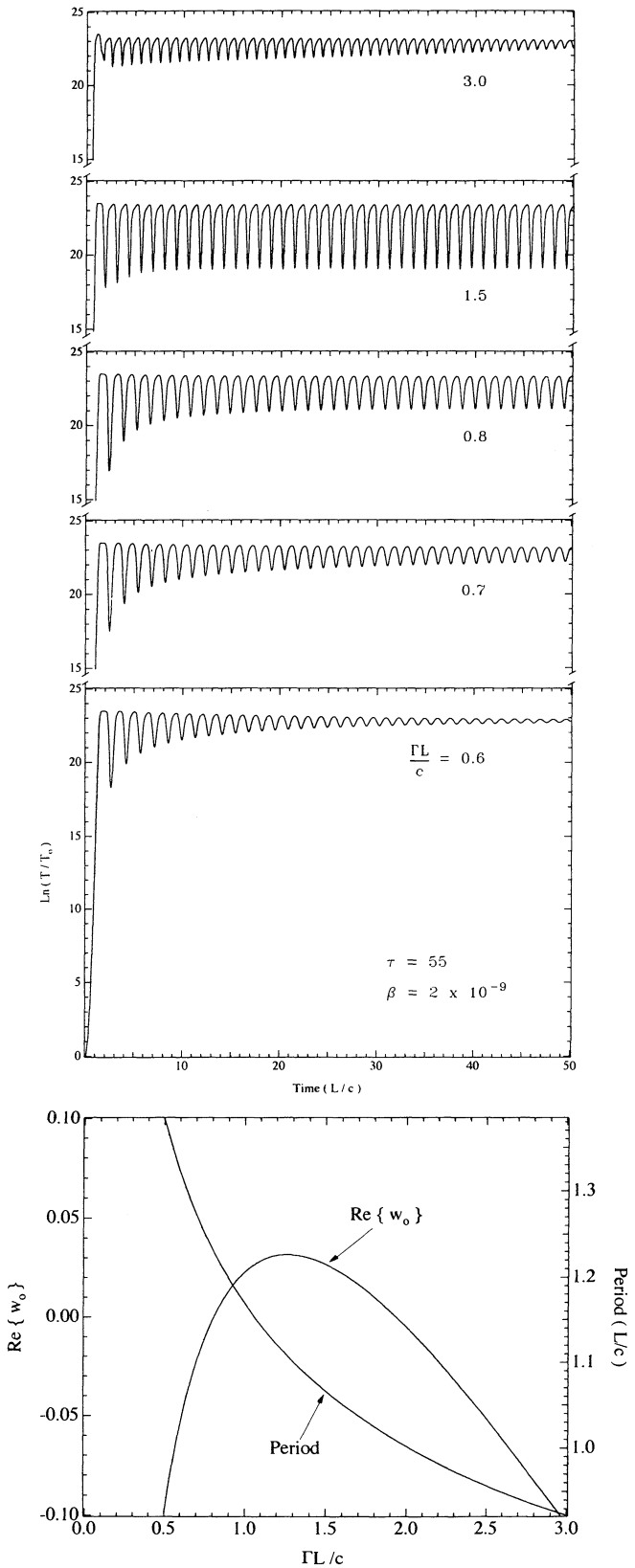

FIG. 6.—Similar to Figs. 1 and 2 except that here the emergent maser intensities from time-dependent calculations are compared with the predictions of the linear stability analysis for several values of $\Gamma L/c$. In the lower panel, the real part of the eigenvalue $w(>0$ for instability) and the period of the oscillation that are obtained from the linear stability analysis are presented as a function of $\Gamma L/c$. The pumping is turned on instantaneously in the time-dependent calculations and $R/\Gamma \simeq 10$.

even though there are two other possibilities. Only for $\Gamma L/c = 15$ where $\mathrm{Re}\,(w) < 0$ for the $0.6L/c$ mode does the system choose a different asymptotic solution. The periodic oscillations in Figure 7*j* thus correspond to the mode with a period of $0.36L/c$ that is identified in Figure 8. In Figures 9 and 10, we show how the asymptotic solutions for the brightness temperature and the eigenvalues from the stability analysis are altered when the separations between the masing components are larger and smaller than in the computations for Figure 7 and 8. At the larger separations as represented by Figure 9, the array of possible behaviors for the system becomes even richer. At the smaller separation, there is only one unstable mode as in the case for a single maser. As was demonstrated for a single maser in Figure 6, there is complete agreement in Figures 8, 9, and 10 between the predictions of the stability analysis and the occurrence of permanent oscillations in the intensity of the emergent maser radiation. When there are many unstable modes indicated in the stability analysis, the system does in fact evolve to a number of asymptotic states depending upon the exact values of the parameters—here, $\Gamma L/c$. The amplitudes as well as the periods for the oscillations vary. In choosing its asymptotic mode for oscillation, the system chooses a period that corresponds closely to that of the unstable mode at the particular value for $\Gamma L/c$ which has the longest period. We have not so far identified a predictable pattern for the periods of the unstable modes. We note that there is a mode in each of these figures for which the period corresponds closely to the combined length of the two masing components divided by the speed of light. In Figures 8 and 10, it is the $0.2L/c$ and $0.5L/c$ modes and is stable. In Figure 9, it presumably is the $0.11L/c$ mode and is slightly unstable.

For the configurations in which the components are well separated (Figs. 7, 8, and 9), we find that the instability tends to disappear when τ for the separate components differs by more than a factor of 3.

4. DISCUSSION

The main new information beyond the stability analysis of SW which is obtained by solving the full, time-dependent equations for the linear maser is that the variation in the intensity of an idealized masing tube can be large—typically one-to-two orders-of-magnitude. At a time long after changes in the physical conditions of the masing gas, the intensity of the maser is found to oscillate permanently. There is agreement in detail for the values of relevant parameters of the masers for which the permanent oscillations occur and for which instability is predicted based on the analysis of small perturbations of the steady state. There also is unexpected agreement in detail between the periods of the permanent oscillations and the periods of the unstable modes found in the stability analysis. When two separated masing regions interact, a number of perods are possible for the oscillations before the permanent, periodic oscillations are dominant. The fluctuations can be irregular for long intervals of time. Likely changes in the physical conditions of the masing gas due to external causes probably occur over time intervals that are much longer than the periods for the maser oscillations. In such cases, the time in which the maser variations are irregular is so long that another external change may occur before the asymptotic, regular oscillatory behavior is achieved. These are probably just glimpses of the arrray of the time variations of the maser intensity that can occur in actual astrophysical environments. A number of masing components (or spots) with different lengths L probably are contributing in the observations, especially in the single-dish measurements. Interactions of maser radiation

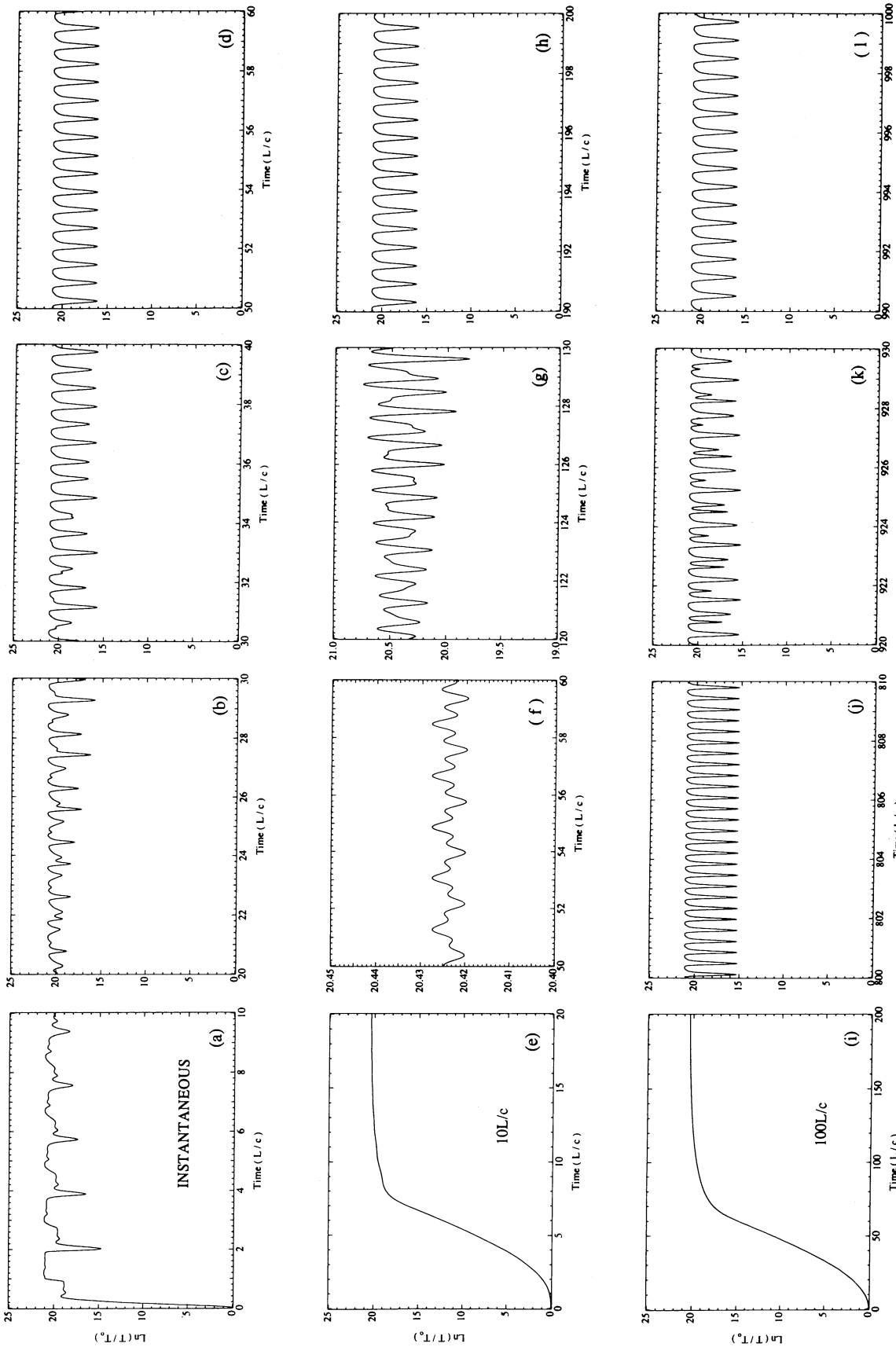

FIG. 7.—Similar to Fig. 1 except that here the intensities are calculated for two identical masing regions that are aligned and interact through their maser radiation. For these calculations, the distance between the outer ends of the two masing regions is L and each maser has a length $0.1L$; the inner edges of the two regions are thus separated by a distance $0.8L$. The optical depth parameter for *each* masing region is 25 so that the steady state solutions are the same as for a single maser with $\tau = 50(R/\Gamma \simeq 7)$. The other parameters are $\beta = 2 \times 10^{-8}$ and $\Gamma L/c = 5$. Masing is initiated by turning on the pumping instantaneously, and over characteristic time scales of $10L/c$ and $100L/c$.

between the masing components may involve more than two components. Velocity gradients, rather than the actual spatial extent of the gas, probably determine the effective lengths L of the masing paths. When velocity gradients, polarization and Zeeman splittings, frequent external perturbations, multiple components, radiative interactions involving several components, etc., are considered, it should not be surprising if the simple periodic oscillations found in our calculations after a long time are not actually observed. Instead, the result that the

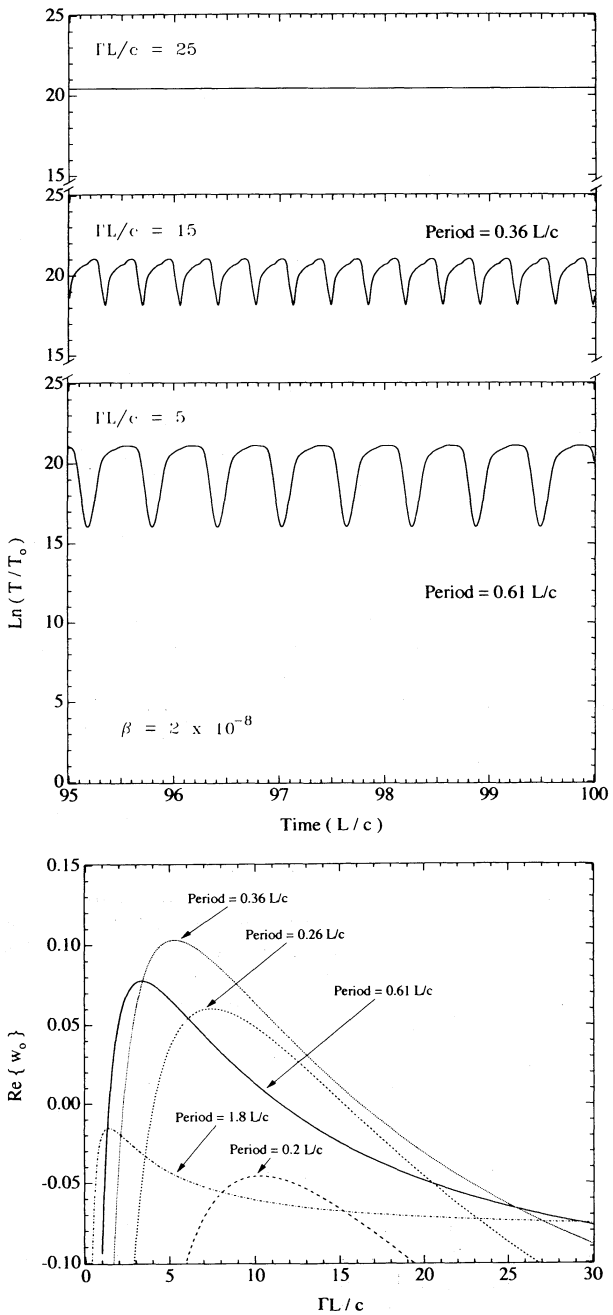

FIG. 8.—A comparison similar to that in Figure 6 of the emergent maser intensities obtained from the time-dependent calculation with the results of the stability analysis for the eigenvalues, for several choices for $\Gamma L/c$ and for the interacting pair of masers considered in Fig. 7. The period associated with each eigenvalue is indicated.

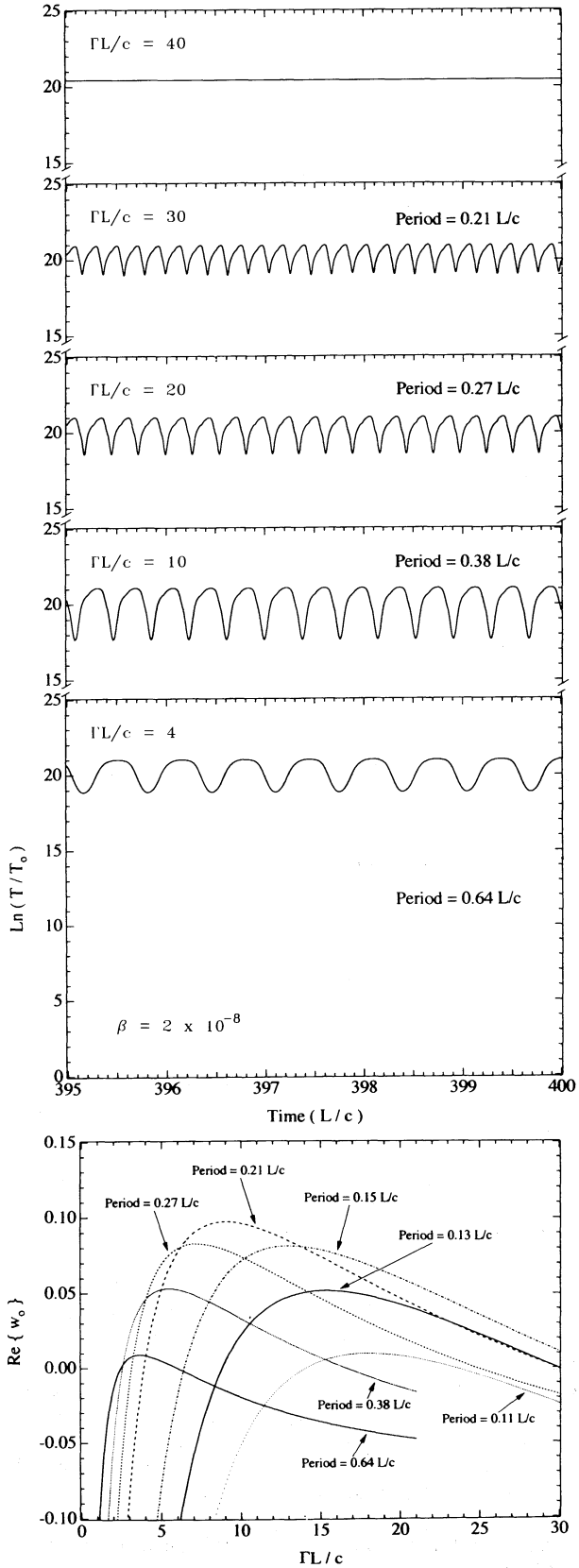

FIG. 9.—Same as Fig. 8 except that here length of each masing region is $0.05L$ so that the separation is $0.9L$. The optical depth parameter is $\tau = 25$ in each region as in Fig. 8.

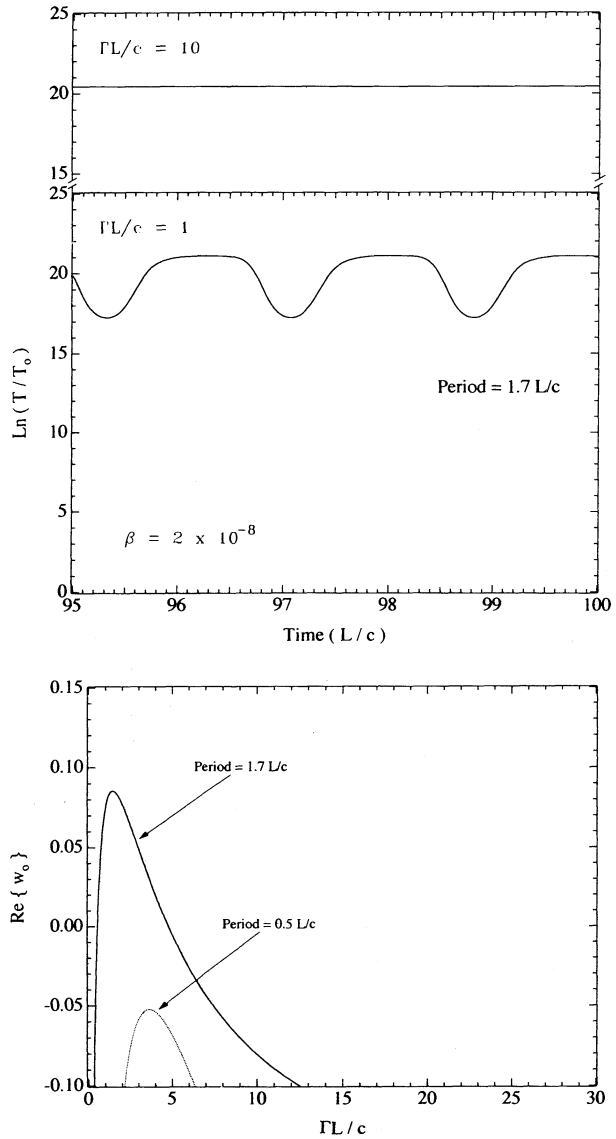

FIG. 10.—Same as Fig. 8, except that here the length of each masing region is $0.25L$ so that the separation is $0.5L$. The optical depth parameter is $\tau = 25$ in each region as in Figs. 8 and 9.

underlying instability can lead to variations of large amplitude for an idealized masing tube provides the basis to believe that perceptible fluctuations can remain after various complicating factors are included.

The parameters that govern the time variations of the maser radiation are exactly the same as those that determine instability in the linear stability analysis—β, τ, $\Gamma L/c$, and $(h\nu/2kT_0)\rho_s$. We have discussed previously (SW) that plausible choices for the incident continuum radiation T_0, the beaming angle $\Delta\Omega$ for the maser, the degree of saturation, the phenomenological decay rate Γ and the factional inversion $\Delta\Lambda/\Lambda$ in the pumping can lead to values of the key parameters for which the interstellar 1665 MHz OH masers are unstable. Inferences that the beaming angles can be quite small ($\gtrsim 10^{-4}$–10^{-5} sr; Nedoluha & Watson 1991) for astrophysical masers bear on the likelihood for instabilities, and on the plausibility of separated, interacting components of masers (Deguchi & Watson 1989). Recent calculations for the pumping of the OH masers also are compatible with $\rho_s \gtrsim 100$ (Field 1985; Cesaroni & Walmsley 1991). The characteristic lengths which seem to be required for at least some masing components to yield 10^3 s fluctuations imply sizes that are somwhat smaller than the commonly accepted values. However, recent studies of interstellar scattering indicate that the true sizes of the 18 cm, interstellar OH masers are significantly smaller than the observed sizes (Diamond et al. 1988; Gwinn et al. 1988). Furthermore, the calculations presented in Figure 2 of SW suggest that in more realistic (two-dimensional) calculations, the restriction to very small $\Delta\Omega$ (and the implied small sizes) may be relaxed. Recent studies (Gaume & Mutel 1987) reinforce the idea that the interstellar OH masers are located preferentially around the edges, and not in front of, the H II regions. Brightness temperatures $T_0 \lesssim 100$ K which are comparable at both ends of the maser are then reasonable. The requirement for comparable incident intensities at both ends may be relaxed when additional considerations such as velocity gradients, several interacting components and multiple masing transitions are included. If some fluctuating masers are directly in front of optically thick H II regions, the continuum radiation from the H II region is much stronger than the radiation from the opposite direction. More complicated geometrical configurations may still be unstable in this case. The phenomenological decay rates Γ for astrophysical masers are commonly approximated by the values of the Einstein A-coefficients for the infrared transitions that connect the masing states to other states Thus, $\Gamma \simeq 0.03\ s^{-1}$ has been adopted for the 18 cm OH masers (e.g., Reid & Moran 1981). However, the same trapping of the infrared radiation that causes the relaxation of the molecular velocities also suppresses the decay of the inverted population due to infrared transitions. Hence, Γ can be much less than the value of the A-coefficients and in the neighborhood of the $10^{-3}\ s^{-1}$ that seems most appropriate for the observed fluctuations. It may be determined by collisions and thus may vary with the number density of the gas. The influence of optical depth effects in suppressing the contribution of the infrared transitions to the value of Γ has been demonstrated explicitly in detailed calculations for the 22 GHz water masers (Anderson & Watson 1992). When the pumping is the greatest in these masers, collisions dominate and yield $\Gamma \simeq 0.1\ s^{-1}$.

Consider now, in detail, how the characteristics of the 1665 MHz masers are compatible with the requirements for radiative instability that have been delineated in our calculations to this point. A common feature of both the individual and pairs of masers is that the minimum period for the oscillations is roughly the length L_0 of the actual masing region divided by the speed of light. The time scale for fluctuations reported by Clegg & Cordes (1991) is the time interval for a change by certain amount from a current value of the intensity. It probably would be about one-fourth of the period for the oscillations if the actual variation were periodic. Radiative instabilities in a length of masing gas $L_0 \approx 1.2 \times 10^{14}$ cm would thus yield fluctuations on a time scale of ~ 1000 s in the observations. In the calculations for both the individual and pairs of masers, the range of Γ for instability seems to be given by $1/2 \lesssim \Gamma L_0/c \lesssim 2$–$3$. With $\Gamma \approx 10^{-3}\ s^{-1}$ and the above value for L_0, $\Gamma L_0/c \simeq 4$ and (within the uncertainties) is compatible with instability. Both individual (see Fig. 2 of SW) and pairs of masers are unstable when the parameter β is smaller than $\sim 10^{-8}$. For $\Gamma = 10^{-3}$ and $T_0 = 100$ K, this requires $\Delta\Omega \lesssim 10^{-3}$ sr. The resulting diameter of an individual masing

cylinder must then be less than $\sim 4 \times 10^{12}$ cm. Although this is considerably smaller than the observed sizes, the effects of interstellar scattering are significant and uncertain. Such sizes, at least for components representing 10% of the power, seem to be plausible. For pairs of interacting masers, the diameters implied by $\Delta\Omega \lesssim 10^{-3}$ sr easily are compatible with expected sizes. For example, for the configuration treated in Figure 9 where $L = 10L_0$, the implied diameter of one of the masing components would be $\sim 4 \times 10^{13}$ cm. The third requirement for instability is an appropriate degree of saturation which we express as the condition that the optical depth parameter $\tau \sim 50$–100. For a spectral line breadth of 0.5 km s^{-1} and assuming that all of the OH is in the four energy levels of the ground rotational state, we can express the optical depth of the 1665 MHz transition of OH as

$$\tau = 6.2 \times 10^{-14}(0.08/-T_x)(\mathrm{OH/H})N_{\mathrm{H}} L_0 \, . \qquad (17)$$

Here, T_x is the negative excitation temperature in kelvins of the 1665 MHz transition, (OH/H) is the fractional abundance of OH molecules, and N_{H} is the number density (cm^{-3}) of hydrogen. The quantity $(0.08/-T_x)$ is also the fractional inversion due to the pumping. Adopting a fractional inversion of a few percent and $N_{\mathrm{H}} \simeq 2 \times 10^{7}$ cm^{-3} (e.g., Cesaroni & Walmsley 1991) together with (OH/H) $\approx 10^{-5}$ gives the necessary optical depth when $L_0 \approx 1.2 \times 10^{14}$ cm in equation (17). Pumping of 1665 MHz masers is a longstanding issue, and it will be surprising if there are not further modifications with the possible results that N_{H} can be increased. In summary, the characteristics of the interstellar 1665 MHz masers are in reasonable agreement with the requirements for instability that have been obtained in our calculations to date. We expect that the additional considerations mentioned in the foregoing may lead to some alterations, at least in detail.

The calculations are equally applicable to masing transitions of other molecules and to other masing transitions of OH when the appropriate values for the four key parameters are determined for these applications (assuming that the simplification $g_u = g_l$ is unimportant). Instabilities of the type described here seem less likely for the masing transitions at higher frequencies because of the effect of spontaneous emission. The $(h\nu/2kT_0)$ in this term will probably be larger by a factor of 100 than for the OH 18 cm masers. Clegg & Cordes (1991) do not find the rapid fluctuations in the circumstellar OH masers at 1665 MHz. Only modest differences in the four key parameters from those of the interstellar masers are required in order that the circumstellar masers be stable. A larger beaming angle $\Delta\Omega$ for the circumstellar masers is one possibility.

In the idealization of these calculations, the fluctuations at all frequencies within a spectral line of a single masing component (or "spot") are correlated. Clegg & Cordes (1991) do report that the fluctuations within the observable spectral lines are correlated. This might not have been the case since a number of separate masing spots with similar velocities (identified by VLBI) frequently are merged in single-dish observations. Separate components may also be merged by interstellar scattering. The highest resolution utilized in observing the fluctuations is 0.11 km s^{-1} and is comparable with the observed breadths when the narrowest components of OH masers are being resolved (e.g., Cohen et al. 1987; Fix 1987; Garcia-Barreto et al. 1988). This resolution also is comparable with the expected widths of individual components as a result of the line narrowing due to saturation, even in the presence of velocity gradients (Nedoluha & Watson 1990). Incorporating additional processes into our calculations such as incomplete relaxation of molecular velocities and velocity gradients may provide the possibility for uncorrelated fluctuations within a spectral line.

Regardless of the particular application to the observations, the investigation here together with that of SW represents a comprehensive, initial analysis of radiative instabilities in astrophysical masers. The basic instability that is recognized here may appear in various forms.

We thank A. W. Clegg, G. E. Nedoluha, and J. M. Stone for helpful discussions during the course of this investigation. Support from NASA Grant NAGW-1104 and NSF Grant AST 89-19614 is gratefully acknowledged.

REFERENCES

Anderson, N., & Watson, W. D. 1992, ApJ, submitted
Bettweiser, E. 1979, A&A, 72, 97
Cesaroni, R., & Walmsley, C. M. 1991, A&A, 241, 537
Clegg, A. W., & Cordes, J. M. 1991, ApJ, 374, 150
Cohen, R. J., Downs, G., Emerson, R., Grimm, M., Gulkis, S., Stevens, G., & Tarter, J. 1987, MNRAS, 225, 491
Deguchi, S. 1974, PASJ, 26, 437
Deguchi, S., & Watson, W. D. 1989, ApJ, 340, L17
Diamond, P. J., Martinson, A., Dennison, B., Booth, R. S., & Winnberg, A. 1988, in AIP Conf. Proc. 174. Radio Wave Scattering in the Interstellar Medium ed. J. M. Cordes, B. J. Rickett, & D. C. Backer (New York: AIP), 195
Field, D. 1985, MNRAS, 217, 1
Fix, J. D. 1987, AJ., 93, 433
Garcia-Barreto, J. A., Burke, B. F., Reid, M. J., Moran, J. M., Haschick, A. D., & Schlizzi, R. T. 1988, ApJ, 326, 957
Gaume, R. A., & Mutel, R. L. 1987, ApJS, 65, 193
Goldreich, P., & Kwan, J. Y. 1974, ApJ, 190, 27
Gwinn, C. R., Moran, J. M., Reid, M. J., & Schneps, M. H. 1988, ApJ, 330, 817
Nedoluha, G. E. 1990, Ph.D. thesis University of Illinois at Urbana-Champaign
Nedoluha, G. E., & Watson, W. D. 1990, ApJ, 361, 653
———. 1991, ApJ, 367, L63
Reid, M. J., & Moran, J. M. 1981, ARA&A, 19, 231
Salem, M., & Middleton, M. S. 1978, MNRAS, 183, 491
Scappaticci, G. A., & Watson, W. D. 1992a, ApJ, 387, L73 (SW)
———. 1992b, in Astrophysical Masers, ed. A. W. Clegg & G. E. Nedoluha (Berlin: Springer), in press (SW)